Journal of Applied Informatics and Computing (JAIC)
Vol.9, No.5, October 2025, pp. 2171~2178
e-ISSN: 2548-6861

Comparative Analysis Transfer Learning Models for Early Detection of Pneumonia using Chest X-ray Images

Rachmasari Annisa Rida [1]*, Majid Rahardi [2]*
* Informatics, Universitas Amikom Yogyakarta
rachmasari.ar@students.amikom.ac.id [1], majid@amikom.ac.id [2]

Article Info

Article history:

Received 2025-08-20
Revised 2025-09-08
Accepted 2025-09-10

Keyword:

Convolutional Neural Network,
DenseNet121,
Pneumonia Detection,
ResNet50,
Transfer Learning.

ABSTRACT

Pneumonia is a serious respiratory disease that continues to be a major worldwide health issue, especially in nations that are struggling with limited medical resources. Early and accurate detection is essential to improve patient outcomes and reducing the rate of death. This study compares the performance of two deep learning architectures, DenseNet121 and ResNet50, using transfer learning for pneumonia detection from chest X-ray images. The dataset consists 5,856 images with two classes, NORMAL and PNEUMONIA, split into training 60%, validation 20%, and testing 20%. Pretrained ImageNet weights were used as fixed feature extractors, with a custom classification layers. Evaluation metrics included accuracy, precision, recall, F1-score, and confusion matrix. On the internal test set, DenseNet121 achieved 92% accuracy, with precision 0.79, recall 0.94, and F1-score 0.86 for NORMAL class, and precision 0.98, recall 0.91, and F1-score 0.94 for PNEUMONIA class. ResNet50 reached 81% accuracy, with precision 0.61, recall 0.80, and F1-score 0.70 for NORMAL class, and precision 0.92, recall 0.81, and F1-score 0.86 for PNEUMONIA class. External testing on an independent set of 200 images (100 images per class) yielded 98% accuracy for DenseNet121 and 85% for ResNet50. These results show that DenseNet121 provides better overall performance and lower false-negative risk for pneumonia cases, highlight the potential of DenseNet121 as a foundation for AI-assisted diagnostic tools in clinical practice.

I. INTRODUCTION

Pneumonia is a type of Acute Respiratory Tract Infection (ARI) that significantly impairs lung function. The lungs contain microscopic air sacs, called alveoli, which expand during respiration. In pneumonia cases, these alveoli become filled with pus and fluid, leading to chest discomfort, breathing difficulties, and reduce oxygen absorption [1], [2]. According to the World Health Organization (WHO), pneumonia remains one of the leading causes of mortality worldwide, contributed to 14% of global child mortality in 2019, accounting for approximately 740,180 deaths among children under the age of five. In Indonesia, the Ministry of Health reported 310,871 pneumonia cases in 2022, indicating that the disease remains a critical public health concern [2], [3].

Traditional diagnosis of pneumonia using chest X-ray interpretation requires skilled radiologists and is time consuming, which poses challenges in areas with limited medical resources [1], [4], [5]. The emergence of deep learning, especially Convolutional Neural Network (CNN), has introduced automated methods for interpreting medical images with high accuracy, offering potential to reduce diagnostic time and minimizing human error [1], [6], [7], [8].

Several works have applied ResNet50 and its variants for pneumonia detection, reporting strong performance. Studies have shown that ResNet50 achieved accuracy above 80% to 90% when trained with ImageNet-pretrained weights [13], [16], while other research emphasized its stability across different datasets [14], [15]. Similarity, DenseNet121 has been widely explored due to its dense connectivity, which enhances feature reuse and gradient propagation. Previous studies reported that DenseNet121 achieved up to 97.03%

accuracy with modified architectures [12], while other works confirmed its robustness in pediatric pneumonia datasets [17], [18]. Other architectures such as MobileNetV2 [17], VGG16 [10], [19], EfficientNet [11], and ensemble methods [3] have also been investigated, achieving varying levels of accuracy.

However, there is a research gap because while transfer learning approaches using pretrained models have been widely adopted for pneumonia classification, few studies directly compare the performance of DenseNet121 and ResNet50 under the same experimental conditions. These architectures are widely recognized for their strong feature extraction capabilities. DenseNet121 promotes features reuse and gradients flow through dense connectivity, whereas ResNet50 employs residual connections to address vanishing gradients in deep networks. In addition, this study implements data augmentation techniques such as random flipping, rotation, and zoom to improve generalization and reduce overfitting, which is particularly important given the limited dataset size.

This research aims to fill this gap by conducting a comparative analysis of DenseNet121 and ResNet50 with transfer learning and image augmentation for pneumonia detection from chest X-ray images. The study evaluates both architectures under identical preprocessing, augmentation, and training configurations. Performance is compared using accuracy, precision, recall, F1-score, and confusion matrix on internal and external test datasets. The results are expected to improve understanding of the impact of architectural selection and contribute in the development of reliable and effective AI-assisted systems for early pneumonia identification [18], [19], [20], [21], [22], [23].

II. METHOD

The pneumonia classification process in this study is based on chest X-ray images, which provide detailed visualization of lung structures. The primary objective is to compare the performance of two Convolutional Neural Network architectures, DenseNet121 and ResNet50 by using transfer learning to classify chest X-ray images into NORMAL and PNEUMONIA categories [1], [12], [13]. The workflow includes dataset preparation, preprocessing with augmentation, model construction using transfer learning, learning with a custom learning rate, and evaluation on internal and external test sets [4], [9], [24].

A. Dataset and Data Split

The dataset used in this research was obtained from an open-source Kaggle repository (Chest X-ray Pneumonia Dataset), consisting of 5,856 chest X-ray images, https://www.kaggle.com/datasets/paultimothymooney/chest-xray-pneumonia [1], [6], [25].

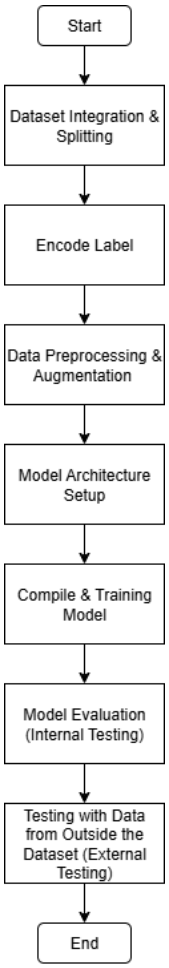

Figure 1. Research flow

The images were divided into two categories, NORMAL and PNEUMONIA. The original distribution was imbalanced, with the PNEUMONIA class having more samples than NORMAL. Although the original Kaggle dataset provides a predefined split for training, validation, and testing, in this study all images were combined into single dataset, then randomly split into training (60%), validation (20%), and testing (20%) to ensure balanced evaluation [22], [24], [26]. An additional external testing dataset comprising 200 images (100 NORMAL and 100 PNEUMONIA) was used to assess generalization performance.

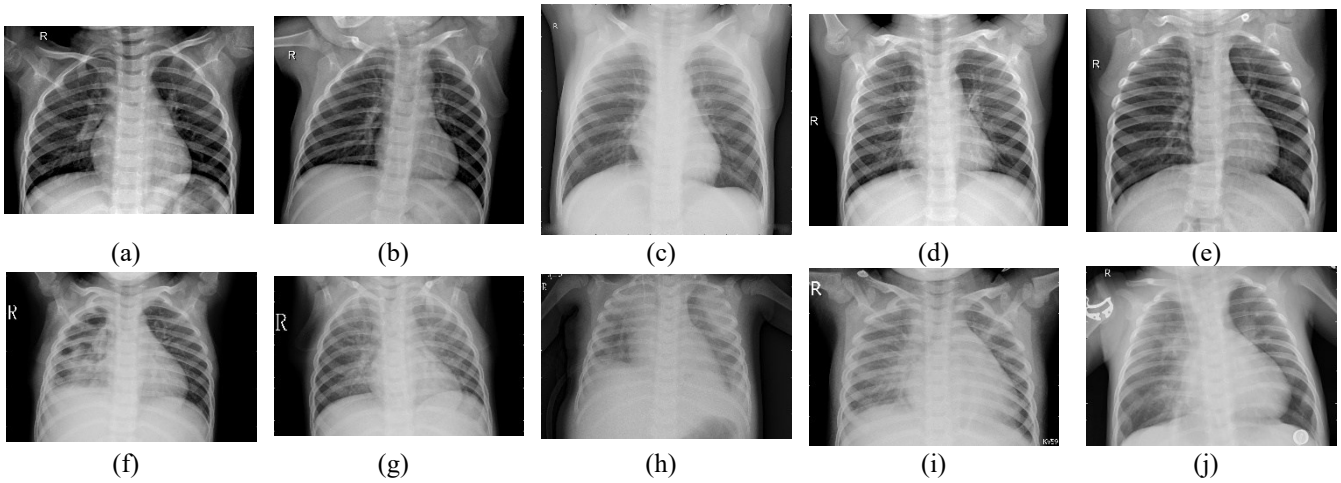

Figure 2. Sample chest X-ray images: (a-e) NORMAL cases, (f-j) PNEUMONIA cases

B. *Preprocessing and Data Augmentation*

All image was resized to 224 x 224 to a pixel values were normalized to a range of 0-1 [7], [18], [24]. Labels were encoded into binary format, with 'NORMAL' assigned a value of 0 and 'PNEUMONIA' assigned a value of 1. Data augmentation was applied only to the training set to improve model generalization and reduce overfitting. The augmentation techniques included random horizontal flipping, random rotation (up to 0.1 radians), and random zoom (up to 0.1 factors). These transformations were implemented using TensorFlow built-in layers within a sequential augmentation pipeline [4], [9], [26].

C. *Model Architecture and Transfer Learning Setup*

Two pretrained convolutional neural network architectures, DenseNet121 and ResNet50, were applied for developing models through transfer learning. Both architectures were initialized with pretrained weights from ImageNet, and configured as frozen feature extractors to retain learned representations from large-scale datasets.

DenseNet121 and ResNet50 were selected because are widely used architectures in medical imaging tasks, offering strong feature extraction capability. DenseNet121 with its dense connectivity, promotes feature reuse and mitigates vanishing gradients issues, making it effective for fine-grained image classification. On the other hand, ResNet50 has a residual block structure that facilitates gradient propagation, which makes training more stable without requiring many additional layers.

A custom classification head was appended to each base model, consisting of a GlobalAveragePooling2D layer to reduce dimensionality, fully connected dense layers with ReLU activation to learn non-linear feature interactions, dropout layers to improve generalization, and a final dense layer with sigmoid activation for binary classification [24], [26]. Both models were compiled using the Adam optimizer for efficient gradient-based optimization, binary crossentropy loss for binary classification, and accuracy as the primary evaluation metric [4], [6], [25].

D. *DenseNet121 Architecture*

DenseNet121 (Densely Connected Convolutional Network) is a deep convolutional neural network designed to improve information flow and gradient propagation by connecting each layer to all subsequent layers within the same dense block [12], [18]. In this study, DenseNet121 was used as the base model with pretrained ImageNet weights to leverage learned representations from large-scale image classification tasks [12], [14], [27]. The classification head comprised GlobalAveragePooling2D layer for feature aggregation, fully connected dense layer with ReLU activation, dropout layers to mitigate overfitting, and a final sigmoid layer for binary classification of NORMAL and PNEUMONIA images [19], [20], [23], [24], [26].

E. *ResNet50 Architecture*

ResNet50 (Residual Network) is a deep convolutional architecture that introduces residual connections, enabling direct pathways for gradients and allowing the network to train efficiently even at greater depths [13], [14]. In this research, ResNet50 was applied as the base model with pretrained weights from ImageNet, configured as a frozen feature extractor to retain general visual features [13], [14]. The top layers were replace with a global average pooling operation, fully connected layers with ReLU activation, dropout layers to reduce overfitting, and a sigmoid output layer to predict the probability of pneumonia from chest X-ray images [16], [24].

F. *Model Training and Evaluation*

Both architectures were compiled using the Adam optimizer with a custom learning rate of 0.0001 to ensure stable convergence during training. Adam optimizer is selected for its adaptive learning rate and efficient gradient-

based optimization. Binary crossentropy was used as the loss function appropriate for binary classification task [4], [9], [24], and accuracy was the primary metric during training [4], [25]. The training process was conducted for 20 epochs with a batch size of 32 on the training set [24], [26]. Data pipelines were optimized using TensorFlow prefetching for efficient GPU utilization.

Model performance was evaluated on an independent test set to assess predictive performance, measured using accuracy, precision, recall, F1-score, and confusion matrix [12], [24]. An additional external testing was carried out on a separate dataset comprising 200 chest X-ray images (100 NORMAL and 100 PNEUMONIA) that were not used in training or validation [12], [14], [16]. This external evaluation aimed to assess the models ability to generalize to unseen data and simulate potential deployment in real clinical scenarios [4], [9], [24].

G. Hardware and Implementation

The experiments were conducted on Google Colab using an NVIDIA Tesla T4 GPU (15GB) with Python 3 runtime. TensorFlow and Keras were used as the primary frameworks for model implementation and training.

Model performance was evaluated using multiple metrics, including accuracy, precision, recall, F1-score, and confusion matrix on both internal and external test datasets. These evaluations aimed to assess not only accuracy but also the model ability to handle class imbalance and minimize false negatives, which is critical for medical diagnosis applications.

III. RESULT AND DISCUSSION

A. Dataset Samples

Figure 2 presents a selection of chest X-ray images from the datasets, including five samples of the NORMAL class and five samples of the PNEUMONIA class. These examples highlight the visual different between healthy lungs and those affected by pneumonia, which the models aim to distinguish.

B. Internal Testing Performance

The evaluation on the internal test set (1,172 images) is summarized in Table I and Table II. DenseNet121 demonstrated superior performance compared to ResNet50 across all metrics.

TABLE I
ACCURACY METRICS DENSENET121

Class	Precision	Recall	F1-Score
NORMAL	0.79	0.94	0.86
PNEUMONIA	0.98	0.91	0.94
Accuracy			0.92

TABLE II
ACCURACY METRICS RESNET121

Class	Precision	Recall	F1-Score
NORMAL	0.61	0.80	0.70
PNEUMONIA	0.92	0.81	0.86
Accuracy			0.81

DenseNet121 outperformed ResNet50 across all evaluation metrics. For NORMAL cases, DenseNet121 achieved a precision of 0.79 and recall of 0.94, while ResNet50 obtained 0.61 precision and 0.80 recall. For PNEUMONIA detection, DenseNet121 reached 0.98 precision and 0.91 recall, compared to ResNet50 with 0.92 precision and 0.81 recall. In addition to precision and recall, the F1-score further highlights the performance gap. DenseNet121 achieved F1-scores of 0.86 for NORMAL and 0.94 for PNEUMONIA, indicating strong consistency between precision and recall. However, ResNet50 recorded significantly lower F1-scores (0.70 for NORMAL and 0.86 for PNEUMONIA), reflecting its difficulty in maintaining a balanced performance, particularly for NORMAL cases.

These results indicate that DenseNet121 not only reduces false negatives but also maintains a balanced trade-off between precision and recall. In contrast, ResNet50 suffered from lower precision for NORMAL cases and higher false negatives for PNEUMONIA, which is critical in clinical settings where missed diagnoses can lead to severe outcomes.

The training and validation accuracy/loss curves (Figure2) indicate stable convergence without signs of overfitting. The confusion matrix (Figure 3) shows that DenseNet121 accurately classified the majority of cases, particularly for pneumonia detection, aligning with findings from prior research where DenseNet121 demonstrated strong feature reuse and gradient propagation for medical imaging.

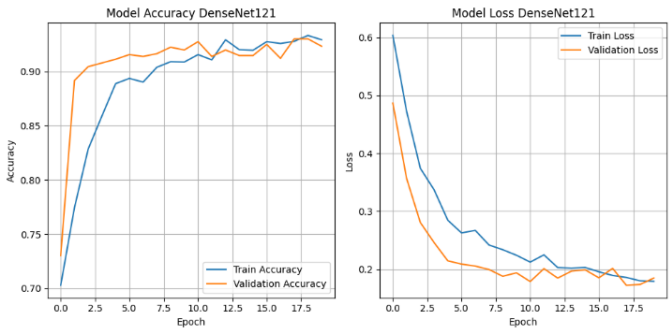

Figure 3. Accuracy and Loss Curves for DenseNet121

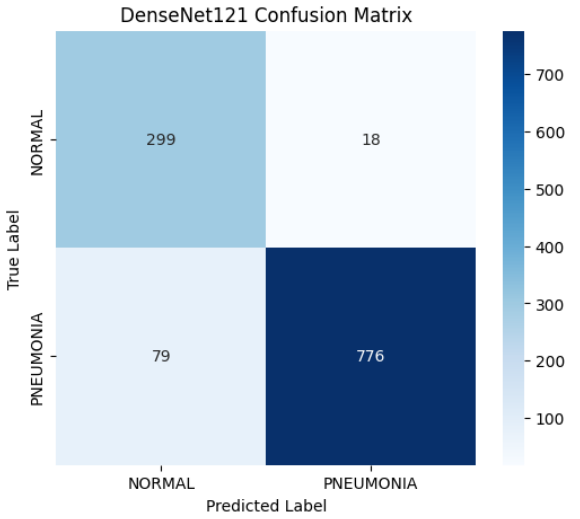

Figure 4. Confusion Matrix for DenseNet121

Performance result demonstrate that ResNet50 achieved competitive performance, although slightly lower in recall and accuracy than DenseNet121 (Figures 4 and 5). This aligns with literature indicating what while ResNet50 benefits from residual connections and robust generalization, DenseNet121 often excels in fine-grained classification tasks due to its dense connectivity.

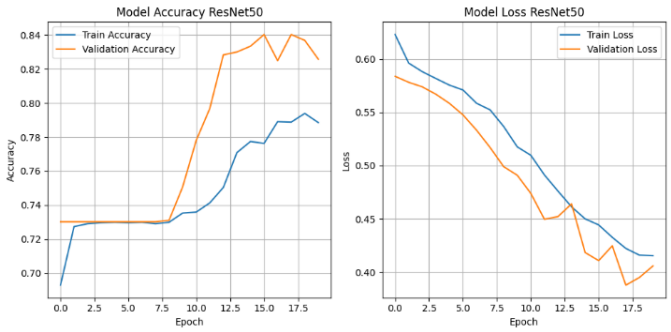

Figure 5. Accuracy and Loss Curves for ResNet50

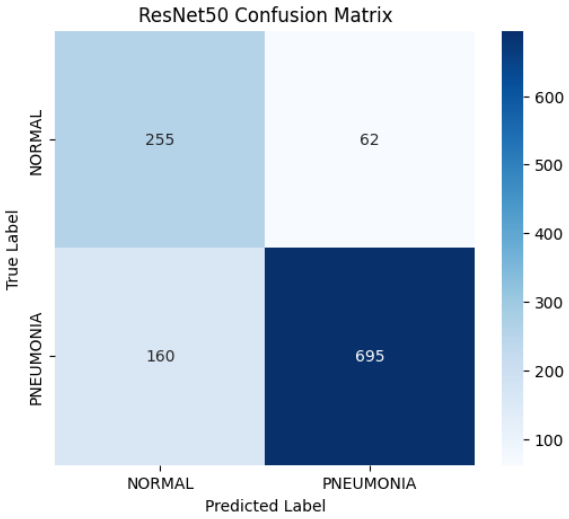

Figure 6. Confusion Matrix for ResNet50

C. *External Testing Analysis*

Generalization performance was evaluated using an external dataset of 200 images (100 NORMAL, 100 PNEUMONIA). The results are shown in Table III.

TABLE III
ACCURACY METRICS DENSENET121 (EXTERNAL TESTING)

Class	Precision	Recall	F1-Score
NORMAL	0.99	0.98	0.98
PNEUMONIA	0.98	0.99	0.99
Accuracy			0.98

TABLE IV
ACCURACY METRICS RESNET121 (EXTERNAL TESTING)

Class	Precision	Recall	F1-Score
NORMAL	0.84	0.87	0.85
PNEUMONIA	0.86	0.83	0.85
Accuracy			0.85

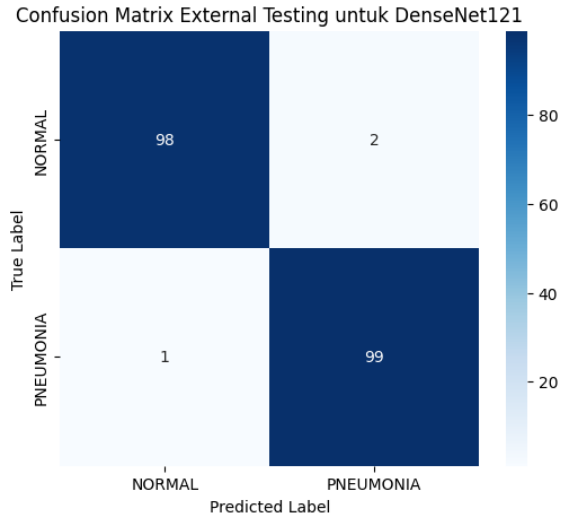

Figure 7. Confusion Matrix External Testing for DenseNet121

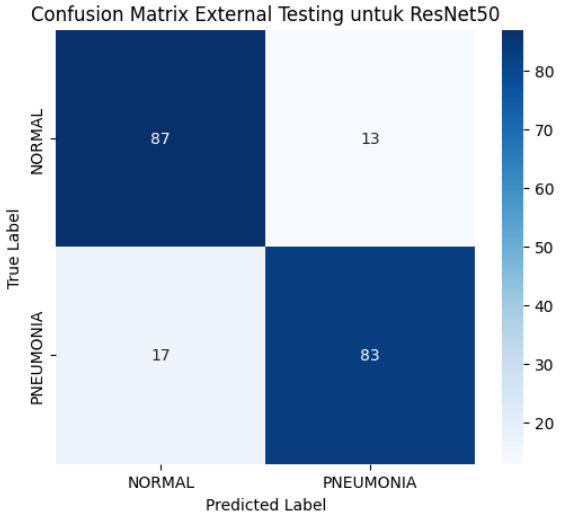

Figure 8. Confusion Matrix External Testing for ResNet50

DenseNet121 delivered near-perfect accuracy on the external dataset, confirming its strong generalization capability. On external data, DenseNet121 maintained both high precision and recall for both classes, with almost perfect scores (precision 0.99 and recall 0.98 for NORMAL; precision 0.98 and recall 0.99 for PNEUMONIA). This indicates strong robustness and adaptability to unseen images. F1-scores on external data reinforce this robustness, with DenseNet121 achieving 0.98 and 0.99 for NORMAL and PNEUMONIA respectively. ResNet50 achieved an F1-score of 0.85 for both classes, confirming its weaker generalization capability. Conversely, ResNet50 showed a noticeable decrease in performance, with recall dropping to 0.83 for PNEUMONIA. This lower sensitivity increases the risk of missed diagnoses, which is critical in medical scenarios where early detection of pneumonia is essential for timely treatment.

D. Comparative Analysis

DenseNet121 consistently achieved the highest accuracy and F1-score both internal and external tests. Its dense connectivity structure allowed efficient feature reuse, contributing to its superior recall for pneumonia detection. The model demonstrated excellent generalization on the external dataset, reaching 98% accuracy. ResNet50 still performing reasonably well, lagged behind DenseNet121 in all metrics. Its accuracy dropped to 81% on the internal test and 85% on the external test. The high number of false negatives for pneumonia in both tests indicates a significant clinical risk. However, ResNet50 remains computationally lighter and faster to train. Training time per epoch for DenseNet121 ranged from approximately 81-83 seconds after the first epoch, compared to 65-84 seconds for ResNet50, confirming that ResNet50 is slightly more efficient in terms of computational.

E. Discussions

The architectural configuration of both models, incorporating GlobalAveragePooling2D, dense layers, and dropout layers, played a critical role in achieving a balance between feature learning and generalization. The GlobalAveragePooling2D layer helped reduce the number of trainable parameters by condensing high-dimensional features from the backbone, while dense layers enabled non-linear transformations to form more discriminative boundaries. Dropout regularization contributed to model robustness by mitigating overfitting, ensuring stability across epochs.

Overall, transfer learning using DenseNet121 and ResNet50 demonstrated competitive performance in pneumonia detection, consistent with previous studies that emphasize the effectiveness of pretrained deep CNNs for medical imaging tasks. The dense connectivity of DenseNet121 significantly improved feature propagation and gradient flow, which explains its superior accuracy and F1-scores compared to ResNet50. Furthermore, the F1-score analysis highlights overall reliability. While accuracy alone might suggest acceptable performance for ResNet50, its lower F1-score for NORMAL cases (0.70) indicates an imbalance between precision and recall, leading to a higher false positive rate. DenseNet121, in contrast, maintained high F1-scores across both classes, confirming its ability to provide consistent and clinically reliable predictions.

From clinical perspective, low false negative rate from DenseNet121 is critical, as misclassifying pneumonia as normal could delay treatment. However, this benefit comes at the cost of higher computational requirements and slightly longer training time per epoch compared to ResNet50 (approximately 81-83 seconds versus 65-84 seconds). In terms of computational trade-off, DenseNet121 achieved higher predictive performance but required slightly longer training time compared to ResNet50. Although ResNet50 is faster and lighter, it might pose a higher diagnostic risk due to its reduced sensitivity to pneumonia cases.

IV. CONCLUSION

This study presents a comparative analysis of two Convolutional Neural Network (CNN) architectures, DenseNet121 and ResNet50, for pneumonia detection using chest X-ray images with transfer learning. The results demonstrate that DenseNet121 achieved superior performance across all evaluation metrics. On the internal test sets, DenseNet121 reached 92% accuracy with precision of 0.79 and recall of 0.94 for NORMAL, and precision of 0.98 and recall of 0.91 for PNEUMONIA, resulting in F1-scores of 0.86 and 0.94 respectively. ResNet50 achieved 81% accuracy with lower performance for NORMAL (precision 0.61, recall 0.80, F1-score 0.70) and moderate results for PNEUMONIA (precision 0.92, recall 0.81, F1-score 0.86). On external testing, DenseNet121 maintained excellent generalization with 98% accuracy, recall and F1-scores of

0.98 and 0.99 for NORMAL and PNEUMONIA, and precision of 0.99 and 0.98. Whereas ResNet50 reached 85% accuracy with precision of 0.84 and 0.86, recall of 0.87 and 0.83, and F1-scores of 0.85 for both classes.

While no formal statistical significance test was conducted, the large performance gap observed between DenseNet121 and ResNet50 (13% accuracy difference and substantially higher F1-score) strongly indicates a meaningful difference in model capability. These findings indicate that DenseNet121 offers a more reliable and clinically applicable solution for early detection.

The research findings affirm that transfer learning without fine-tuning can provide effective results for medical image classification, particularly when the available training data is limited. The use of pretrained models accelerates development time while still yielding high accuracy in classifying pneumonia cases. Moreover, the external testing conducted using 200 independent images (100 per class) demonstrates the model's ability to generalize to unseen data. This result suggest that transfer learning is a promising approach for rapid deployment in medical imaging analysis systems.

However, this study has several limitations, including only two classes in the dataset, there is no fine-tuning process on the previously trained model, and the limited amount of data used during external testing. For future research, incorporating fine-tuning techniques by unfreezing selected layers of the pretrained models could be explored to enhance feature learning. In addition, combining advanced augmentation techniques, ensemble approaches, or experimenting with other architectures such as EfficientNet or InceptionV3 may further improve detection accuracy. Expanding evaluation to include computational efficiency metrics and robustness testing under various image quality conditions is also recommended for practical clinical application. The implementation of this system can serve as a foundation for developing AI-assisted diagnostic tools in clinical settings, especially in areas with limited medical resources and radiological expertise.

REFERENCES

[1] S. G. Gundabatini, "Pneumonia Detection using CNN, Resnet and DenseNet," *Int. J. Res. Appl. Sci. Eng. Technol.*, vol. 12, no. 3, pp. 1680–1686, 2024, doi: 10.22214/ijraset.2024.59145.

[2] E. Longjiang *et al.*, "Image-based deep learning in diagnosing the etiology of pneumonia on pediatric chest X-rays," *Pediatr. Pulmonol.*, vol. 56, no. 5, pp. 1036–1044, 2021, doi: 10.1002/ppul.25229.

[3] W. Akbar *et al.*, "Pneumonia Detection: A Comprehensive Study of Diverse Neural Network Architectures using Chest X-Rays," *Int. J. Appl. Math. Comput. Sci.*, vol. 34, no. 4, pp. 679–699, 2024, doi: 10.61822/amcs-2024-0045.

[4] A. W. Salehi, S. Khan, G. Gupta, B. I. Alabduallah, and A. Almjally, "Cnn1.Pdf," 2023.

[5] P. Szepesi and L. Szilágyi, "Detection of pneumonia using convolutional neural networks and deep learning," *Biocybern. Biomed. Eng.*, vol. 42, no. 3, pp. 1012–1022, 2022, doi: 10.1016/j.bbe.2022.08.001.

[6] O. Iparraguirre-Villanueva, V. Guevara-Ponce, O. R. Paredes, F. Sierra-Liñan, J. Zapata-Paulini, and M. Cabanillas-Carbonell, "Convolutional Neural Networks with Transfer Learning for Pneumonia Detection," *Int. J. Adv. Comput. Sci. Appl.*, vol. 13, no. 9, pp. 544–551, 2022, doi: 10.14569/IJACSA.2022.0130963.

[7] D. Nurhamzah, I. W. Sariyanto, N. Luh, and G. Pivin, "Identifikasi Pneumonia pada Citra Rontgen Paru-paru Menggunakan Convolutional Neural Network," vol. 1, no. 3, pp. 72–77, 2024.

[8] B. F. H. Irfan Handy Office, Rahman Arifuddin, "Klasifikasi Pneumonia menggunakan Metode Convolutional Neural Network," *Techné J. Ilm. Elektrotek.*, vol. Vol.23, no. No.2, pp. 233–244, 2024.

[9] Z. Zhao, L. Alzubaidi, J. Zhang, Y. Duan, and Y. Gu, "A comparison review of transfer learning and self-supervised learning: Definitions, applications, advantages and limitations," *Expert Syst. Appl.*, vol. 242, no. December 2023, p. 122807, 2024, doi: 10.1016/j.eswa.2023.122807.

[10] M. Idhom, D. A. Prasetya, P. A. Riyantoko, T. M. Fahrudin, and A. P. Sari, "Pneumonia Classification Utilizing VGG-16 Architecture and Convolutional Neural Network Algorithm for Imbalanced Datasets," *TIERS Inf. Technol. J.*, vol. 4, no. 1, pp. 73–82, 2023, doi: 10.38043/tiers.v4i1.4380.

[11] A. Alghanmi, "An Accurate Pneumonia Detection Scheme Using Hybrid Algorithms," *Math. Model. Eng. Probl.*, vol. 12, no. 2, pp. 676–686, 2025, doi: 10.18280/mmep.120231.

[12] T. S. Arulananth, S. W. Prakash, R. K. Ayyasamy, V. P. Kavitha, P. G. Kuppusamy, and P. Chinnasamy, "Classification of Paediatric Pneumonia Using Modified DenseNet-121 Deep-Learning Model," *IEEE Access*, vol. 12, no. March, pp. 35716–35727, 2024, doi: 10.1109/ACCESS.2024.3371151.

[13] H. D. Hekmatyar, W. A. Saputra, and C. Ramdani, "Klasifikasi Pneumonia Dengan Deep Learning Faster Region Convolutional Neural Network Arsitektur VGG16 dan ResNet50," *InComTech J. Telekomun. dan Komput.*, vol. 12, no. 3, p. 186, 2022, doi: 10.22441/incomtech.v12i3.15112.

[14] A. Victor Ikechukwu, S. Murali, R. Deepu, and R. C. Shivamurthy, "ResNet-50 vs VGG-19 vs training from scratch: A comparative analysis of the segmentation and classification of Pneumonia from chest X-ray images," *Glob. Transitions Proc.*, vol. 2, no. 2, pp. 375–381, 2021, doi: 10.1016/j.gltp.2021.08.027.

[15] T. Berliani, E. Rahardja, and L. Septiana, "Perbandingan Kemampuan Klasifikasi Citra X-ray Paru-paru menggunakan Transfer Learning ResNet-50 dan VGG-16," *J. Med. Heal.*, vol. 5, no. 2, pp. 123–135, 2023, doi: 10.28932/jmh.v5i2.6116.

[16] C. Neural, "Pneumonia Detection Through CNN and Resnet-50 1 Introductions 2 Related work," vol. 8, no. 1, pp. 64–72, 2025.

[17] P. Mobilenetv and D. A. N. Densenet, "Perbandingan mobilenetv2 dan densenet121 pada klasifikasi terumbu karang menggunakan convolutional neural network," vol. 2, no. 3, pp. 930–941, 2025.

[18] A. A. Khan *et al.*, "Detection of Omicron Caused Pneumonia from Radiology Images Using Convolution Neural Network (CNN)," *Comput. Mater. Contin.*, vol. 74, no. 2, pp. 3743–3761, 2023, doi: 10.32604/cmc.2023.033924.

[19] Dr. Sunil L. Bangare, Hrushikesh S. Rajankar, Pavan S. Patil, Karan V. Nakum, and Gopal S. Paraskar, "Pneumonia Detection and Classification using CNN and VGG16," *Int. J. Adv. Res. Sci. Commun. Technol.*, no. May, pp. 771–779, 2022, doi: 10.48175/ijarsct-3851.

[20] M. Bundea and G. M. Danciu, "Pneumonia Image Classification Using DenseNet Architecture," *Inf.*, vol. 15, no. 10, 2024, doi: 10.3390/info15100611.

[21] A. Çı, M. Yıldırı, and Y. Eroğlu, "Traitement du Signal Classification of Pneumonia Cell Images Using Improved ResNet50 Model," *Int. Inf. Eng. Technol. Assoc.*, vol. 38, no. 1, pp. 165–173, 2021.

[22] M. Harahap, Em Manuel Laia, Lilis Suryani Sitanggang, Melda Sinaga, Daniel Franci Sihombing, and Amir Mahmud Husein, "Deteksi Penyakit Covid-19 Pada Citra X-Ray Dengan Pendekatan

Convolutional Neural Network (CNN)," *J. RESTI (Rekayasa Sist. dan Teknol. Informasi)*, vol. 6, no. 1, pp. 70–77, 2022, doi: 10.29207/resti.v6i1.3373.

[23] F. Z. Hamlili, M. Beladgham, M. Khelifi, and A. Bouida, "Transfer learning with Resnet-50 for detecting COVID-19 in chest X-ray images," *Indones. J. Electr. Eng. Comput. Sci.*, vol. 25, no. 3, pp. 1458–1468, 2022, doi: 10.11591/ijeecs.v25.i3.pp1458-1468.

[24] A. H. Alharbi and H. A. Hosni Mahmoud, "Pneumonia Transfer Learning Deep Learning Model from Segmented X-rays," *Healthc.*, vol. 10, no. 6, 2022, doi: 10.3390/healthcare10060987.

[25] Q. An, W. Chen, and W. Shao, "A Deep Convolutional Neural Network for Pneumonia Detection in X-ray Images with Attention Ensemble," *Diagnostics*, vol. 14, no. 4, pp. 1–23, 2024, doi: 10.3390/diagnostics14040390.

[26] J. Colin and N. Surantha, "Interpretable Deep Learning for Pneumonia Detection Using Chest X-Ray Images," *Inf.*, vol. 16, no. 1, 2025, doi: 10.3390/info16010053.

[27] Q. Zhou, W. Zhu, F. Li, M. Yuan, L. Zheng, and X. Liu, "Transfer Learning of the ResNet-18 and DenseNet-121 Model Used to Diagnose Intracranial Hemorrhage in CT Scanning," *Curr. Pharm. Des.*, vol. 28, no. 4, pp. 287–295, 2021, http://dx.doi.org/10.2174/1381612827666211213143357.